Available online at www.sciencedirect.com

ScienceDirect

European Polymer Journal 43 (2007) 2191–2206

EUROPEAN POLYMER JOURNAL

www.elsevier.com/locate/europolj

Macromolecular Nanotechnology

Nanostructure vs. microstructure: Morphological and thermomechanical characterization of poly(L-lactic acid)/layered silicate hybrids

Sotirios I. Marras [a,b], Ioannis Zuburtikudis [b,*], Costas Panayiotou [a,*]

[a] *Department of Chemical Engineering, Aristotle University of Thessaloniki, 54124 Thessaloniki, Greece*
[b] *Department of Industrial Design Engineering, TEI of Western Macedonia, 50100 Kozani, Greece*

Received 9 January 2007; received in revised form 23 February 2007; accepted 5 March 2007

Abstract

Nano- and micro-composites of poly(L-lactic acid) (PLLA) with various loadings of natural and hexadecylamine-modified montmorillonite were prepared by the solvent casting method to study the effect of nanostructure on the thermomechanical properties of the hybrid materials. The changes on structure and surface of montmorillonite, induced by the ion-exchange modification process, were characterized by X-ray diffraction (XRD) analysis and zeta-potential determination, while the morphology of the hybrids and the dispersion of the clay into the polymer matrix were examined by XRD, transmission electron microscopy and atomic force microscopy. The results showed that, although at low clay content exfoliation dominates, for filler loadings greater than 5 wt% both exfoliation and intercalation of the clay filler are observed. Thermal degradation studies of the materials produced using thermogravimetry revealed the introduction of a small amount of organo-modified silicate significantly improves their thermal stability. Differential scanning calorimetry showed the thermal behavior of the polymer matrix strongly depends on the nature and content of the silicate filler. Scanning electron microscopy of the deformed surfaces affirmed a different deformation process mechanism between the two types of composites.

Keywords: Biodegradable polymer; Poly(L-lactic acid); Nanocomposites; Thermal properties; Mechanical properties

---

1. Introduction

Polymer nanocomposites are a class of materials that has already gained a big popularity among researchers both in academia and industry due to their exceptional properties, which are superior to those of the virgin polymers and of the conventional composites [1]. These hybrid materials consist of a polymer matrix in which inorganic particles with at least one dimension in the nanometer scale are homogeneously dispersed. The nano-sized particles that are typically less than 5 wt% in proportion interact with the polymer matrix and improve substantially many physical properties of the pristine

---

[*] Corresponding authors. Tel.: +30 24610 40161; fax: +30 24610 39682 (I. Zuburtikudis), tel.: +30 2310 996223; fax: +30 2310 996232 (C. Panayiotou).

E-mail addresses: izub@teikoz.gr (I. Zuburtikudis), cpanayio@auth.gr (C. Panayiotou).

0014-3057/$ - see front matter © 2007 Elsevier Ltd. All rights reserved.
doi:10.1016/j.eurpolymj.2007.03.013

polymer including increased mechanical characteristics [2], enhanced barrier resistance [3], decreased flammability [4,5], and increased biodegradability in the case of biodegradable polymers [6].

Biodegradable and biocompatible polymers have also attracted significant attention in the last decade in general and, more specifically, they have become the polymer matrix of choice for many researchers in the field of nanocomposites; they are environmentally friendly, as they degrade under the action of physicochemical and biological factors in a humid environment, while they can be employed in many biomedical and pharmaceutical applications such as sutures and biologically active controlled-release devices [7]. In this direction, poly(lactic acid) (PLA) is rapidly gaining recognition as one of the most popular biopolymers. It is a linear aliphatic polyester derived from 100% renewable resources such as corn and sugar beets.

PLA can be prepared either by direct condensation of lactic acid or by the ring-opening polymerization of the cyclic lactide dimer [8]. The direct condensation path is an equilibrium reaction causing difficulties in removing trace amounts of water in the late stages of polymerization. For this reason, only a low molecular mass polymer can be obtained by this approach. Three stereoisomers of lactide exist: L-lactide, D-lactide and mesolactide. The stereochemical structure of the lactide monomer determines the stereochemical composition of the resulting polymer. Sequentially, it is the architecture of the resulting polymer (determined by the proportions of L, D, and the molecular mass) that dictates its properties such as crystallinity, melting point, and mechanical strength. Thus, PLA can be totally amorphous or up to 40 % crystalline depending on the proportions of D and L-lactides present [8]. As a consequence, PLA polymers can display a broad range of mechanical properties, their glass transition temperature may range from 50 °C to 80 °C, while their melting point can vary from 130 °C to 180 °C.

As regards the nano-sized inorganic particles that are added in the polymer matrix, phyllosilicates such as montmorillonite clay are of particular interest because of their abundance, low cost and their geometrical features. They consist of numerous layers stacked in parallel, otherwise called ‘‘platelets’’, that are nm-thick and hundreds-nm- or μm-long; that is, each platelet has a high aspect ratio, which enhances the possibility for energy transfer from the inorganic phase to the organic one and vice versa [9]. Natural clays mixed with polymers lead to the formation of nanocomposites very rarely. Their hydrophilic nature obstructs their homogeneous dispersion in the organic polymer phase. However, it is well known [10] for immiscible organic-inorganic systems, that the weak interaction between the organic and the inorganic components results in poor mechanical and thermal properties. In order to render the hydrophilic phyllosilicates more organophilic, hydrated cations (Ca^{++}, Na^{+}) of the interlayer space are exchanged with cationic surfactants such as alkylammonium or alkylphosphonium. This ion-exchange reaction lowers the surface energy of the inorganic material and makes it compatible with organic liquids [11] or polymers [12].

From the structural point of view, two types of polymer/phyllosilicate nanocomposites are possible, the so-called ‘‘intercalated’’ and the ‘‘exfoliated’’ one, although in most of the real cases and unless special care has taken, the usual situation is a mixture of ‘‘intercalated’’ and ‘‘exfoliated’’ nanocomposites [1]. In an intercalated system, the polymer is inserted into the silicate galleries, i.e. the interlayer space, but the stacking of the silicate layers is preserved. In an exfoliated system, the silicate layers are fully separated and randomly dispersed in the polymer matrix due to the extensive polymer insertion [13]. This good dispersion of the clay platelets gives rise to a bigger property enhancement, since the nanostructure effect can be more pronounced in the exfoliated nanocomposite than in the intercalated one.

Polymer/layered-silicates nanocomposites can be prepared by the following methods: (i) Solution-casting, (ii) in situ polymerization, (iii) melt intercalation. In the first case, the inorganic material is thoroughly mixed and dispersed in a polymer solution resulting in the insertion of polymer chains into the galleries of the clay, which swells. In situ polymerization involves monomer intrusion into the clay galleries followed by polymerization. In the melt intercalation process, the molten polymer is blended with the clay, so that the polymer/layered silicate interactions be optimized and the insertion of the polymer chains is facilitated [1].

PLA/layered silicate nanocomposites have been prepared by several methods such as melt extrusion [10,14–16] and solution casting [17–19]. The aim has been to produce a hybrid material with improved properties over pristine PLA. However, many aspects of the composite’s structure-property relationship have not been elucidated yet. Understanding this structure-property relationship thoroughly is the key in designing materials with tailor-made properties. The effect of clay content and the composite's morphology on the physical properties of the hybrid material are two key issues towards this direction.

In the present study, micro- and nanocomposites of poly(L-lactic acid) (PLLA) with various compositions of natural and organophilic montmorillonite clay were prepared by the solution casting method using chloroform as the solvent. The aim was to investigate the role of nanostructure on the thermal and mechanical behavior of the hybrid materials by comparing the thermo-mechanical properties of the nanocomposites with the corresponding ones of the microcomposites.

2. Experimental

2.1. Materials

PLLA ($M_n = 81{,}000$, $M_w/M_n = 1.9$ and 0% content in D-lactide stereoisomer was obtained from Galactic S.A. (Belgium), while sodium montmorillonite (NaMMT) (CEC = 92.6 meq/100 g) was supplied by Southern Clay Products (Texas, USA). Hexadecylamine ($C_{16}A$), chloroform ($CHCl_3$) and concentrated HCl were purchased from Sigma–Aldrich. All materials were used as received and without any further purification.

2.2. Preparation of the organophilic layered silicate

Organically modified montmorillonite ($C_{16}MMT$) was prepared through an ion-exchange reaction between sodium montmorillonite and hexadecylammonium salt ($C_{16}A$). Quantity of $C_{16}A$, equal to 1.4 times the cation exchange capacity (CEC) of the inorganic material and an equivalent amount of HCl were dissolved in a 1:1 solution of ethanol and water at 75 °C. The inorganic material was dispersed in water at 75 °C and then, this aqueous suspension (3 wt%) was added to the alkylammine solution. The mixture was stirred vigorously for 24 h at the aforementioned temperature. The precipitate was collected by filtration and washed with a hot 1:1 solution of ethanol and water until the $AgNO_3$ test verified the absence of chloride. Eventually, the cation-exchanged montmorillonite was dried and ground to a powder, which was kept in a desiccator for further use.

2.3. Preparation of hybrid materials

Nanocomposites were fabricated by using the solution casting technique. Initially, the organo-modified montmorillonite was dispersed in chloroform. The clay suspension was sonicated for 1 h with a Heat Systems-Ultrasonics, W-375 sonicator. Then, the polymer was dissolved in it and the whole dispersed-clay polymer solution (5 wt%) was further sonicated for 1 h. Extended increase of the solution temperature was avoided by using a pulse mode. The mixture was then cast onto Petri dishes and was kept for 48 h in a chloroform atmosphere in order to accomplish a slow solvent evaporation, which eliminates polymer skin formation. Chloroform was selected as the PLLA solvent instead of dichloromethane, because of its lower vapor pressure when compared with dichloromethane and this led to the formation of a more homogeneous film [20]. That way, nanocomposite membranes with organoclay content ranging from 1 to 30 wt% and with thickness between 100 and 150 μm were obtained; these films were eventually dried in vacuum at 50 °C for 24 h.

As written in the introduction, in order to achieve a better understanding of the nanostructure effect on the thermo-mechanical properties of the hybrid materials, microcomposites were also produced by the above described procedure using, however, unmodified sodium montmorillonite. In this case, a smaller number of final hybrid compositions were prepared (1–8 wt% clay), just for the required comparisons.

2.4. Characterization

The electrokinetic potential (ζ) of both the natural, i.e. unmodified clay, and the organophilic one were measured at different pH values using Smoluchowski's equation and with the aid of an automated microelectrophoresis instrument (ZetaPlus, Brookhaven Instruments Corporation). At least 20 runs were conducted for each sample and the average values were recorded. For the preparation of the samples, sufficient amount (2 mg/ml) of dry clay was dispersed in de-ionized water and the suspension was shaken intensively for 24 h. pH adjustment took place by dropwise addition of HCl or NaOH solutions. All measurements were conducted at 23 °C ± 0.2 °C.

The structure of the hybrid materials being either nano- or micro-scaled was investigated by XRD using a Siemens D 500 diffractometer and Ni-filtered Cu Kα radiation ($\lambda = 0.154$ nm). The scanning range was varied from $2\theta = 2°$ to $30°$.

The differences of the clays surface morphology was visualized by using a Jeol JSM-5900 LV scanning electron microscope (SEM). The samples were coated with a carbon thin film under vacuum in an Agar auto carbon coater.

The dispersion of the silicate layers was also evaluated by transmission electron microscopy (TEM) bright field imaging using a Jeol 120CX microscope operating at 120 kV and a JEOL 2011 operating at 200 kV (for higher resolution). Specimens suitable for planar view observations were mechanically thinned down to 10 μm followed by further thinning to electron transparency by Ar ion beam milling at a low incident angle of 5°.

Atomic force microscopy (AFM) measurements were performed on a Veeco, CP-II microscope. The instrument was operated in intermittent-contact mode to eliminate lateral forces, which can damage the sample or the tip and reduce image resolution. Height (topography) and phase images were recorded at room temperature and ambient atmosphere. A commercial silicon tip-cantilever was used with a spring constant 20–80 N/m, a resonance frequency in the 200–400 Hz range and a tip radius of less than 10 nm. For this analysis, smooth cross-sections were made by room temperature microtoming. Usually, the "simply cut" cross sections are too rough to obtain the fine details. The samples were imaged 10 days after micro-cleavage, showing that the sample cross-sections were stable for long time.

The thermal properties of the produced hybrids were investigated with the aid of a Scimadzu DSC-50 differential scanning calorimeter (DSC). Temperature scans were carried out at a heating rate of 10 °C/min under constant nitrogen flow of 20 cm^3/min. The samples were heated to 200 °C and remained at that temperature for 5 min in order to release their thermal history and, afterwards, they were quenched to −5 °C. The determination of the glass transition temperature (T_g), crystallization temperature (T_c) and melting point (T_m) took place during the second run. Thermogravimetric analyses (TGA) of the hybrids were performed on a Shimadzu TGA-50 with a heating ramp of 10 °C/min up to 750 °C under both flowing nitrogen (20 cm^3/min) and static air. TGA runs in isothermal conditions were also conducted at 280 °C in air.

The mechanical properties of the produced composites were studied in tensile loading conditions using a Thumler GmbH Z3-500 tensile tester according to ASTM D1708 method. The crosshead speed was 5 mm/min. At least six measurements were taken for each sample and the results were averaged to obtain a mean value. The surface morphology of the tensile deformed composites and their fracture surface were examined with a scanning electron microscope (SEM). The sample preparation for the SEM examination was similar to that described above.

3. Results and discussion

3.1. Organoclay characteristics

The unit layers of montmorillonite are stacked together face-to-face forming the crystal lattice. The basal spacing (i.e. the distance between two successive plane layers) of both the natural (sodium) montmorillonite and the organically (hexadecylammonium cation) modified montmorillonite was investigated by XRD and the results are presented in Fig. 1. It appears that the basal spacing of the layered mineral is 1.2 nm. Insertion of hexadecylammonium ions into the interlayer spaces of the natural clay led to an increase of this spacing from 1.2 nm to 1.82 nm indicating a bilayer arrangement of the alkylammonium molecules [21,22].

In Fig. 2, the electron photomicrographs taken by the SEM describe the surface characteristics of NaMMT and C_{16}MMT. As observed, the granule of modified montmorillonite exhibits a more open

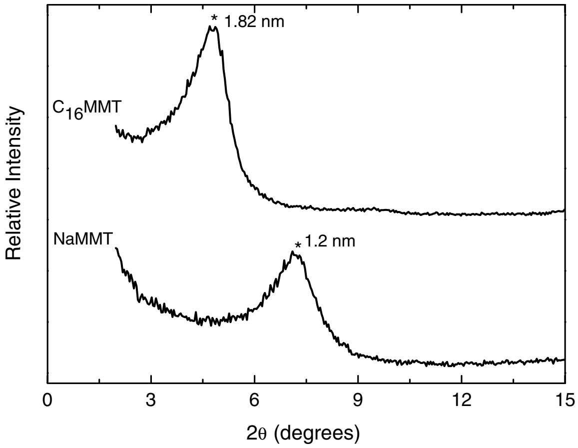

Fig. 1. X-ray diffraction patterns of natural and organo-modified montmorillonite.

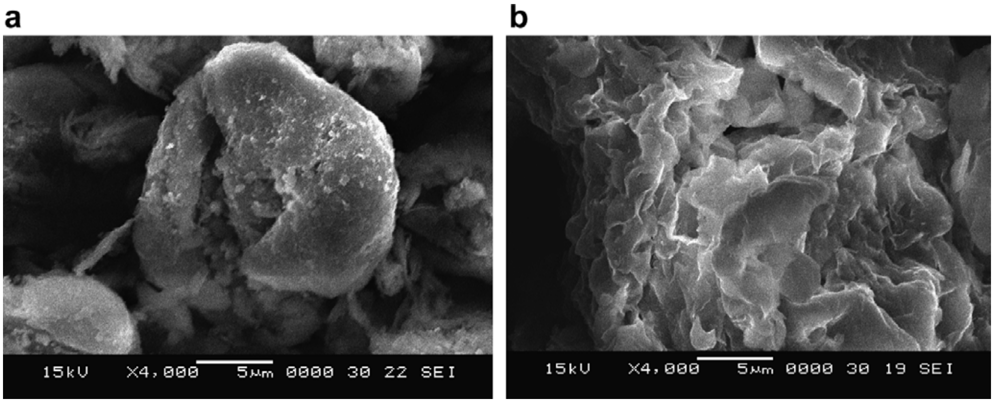

Fig. 2. SEM micrographs of (a) un-modified and (b) modified montmorillonite.

structure, while individual blocks of layers can be distinguished in it.

Fig. 3 illustrates the zeta potential of the clay as a function of the solution's pH. As it is clearly shown, the zeta potential of the natural clay is negative over the whole range of pH values. Moreover, it does not change significantly with pH. These observations are in accordance with Swartzen et al. [23], who have claimed that the surface charge of NaMMT in aqueous solutions is always negative and pH independent due to the isomorphic substitutions of Al^{3+} by Mg^{2+} in the octahedral sheet and those of Si^{4+} by Al^{3+} in the tetrahedral sheet. However, at the edges of the particles where the aluminum hydrosilicate layers are disrupted, polar sites are situated due to broken bonds. These sites are conditionally charged (positively or negatively) by direct H^{+} or OH^{-} transfer from the aqueous phase depending on the pH. Addition of $C_{16}A$ leads to an increase of the surface charge of MMT, which becomes positive in neutral and acidic solutions and decreases as the concentration of the hydroxyl ions is increased. Xu and Boyd [24] proposed that the alkylammonium cation is initially adsorbed in the interlayer space by cation exchange and this causes extensive clay aggregation. Increasing the cation loading, $C_{16}A$ is adsorbed on the external surfaces of the aggregates via both cation exchange and hydrophobic bonding; the hydrophobic bonding causing positive charge development on the surfaces and ultimately clay dispersion. Two types of amine adsorption reactions on montmorillonite were also pointed out by Zhang et al. [25]: cation-exchange reaction and adsorption at non-exchangeable sites with the former to be the dominating reaction, when the amount of amine is less than 100% of the clay CEC. These views are in accordance with all of the experimental findings described in Fig. 3 and explain them.

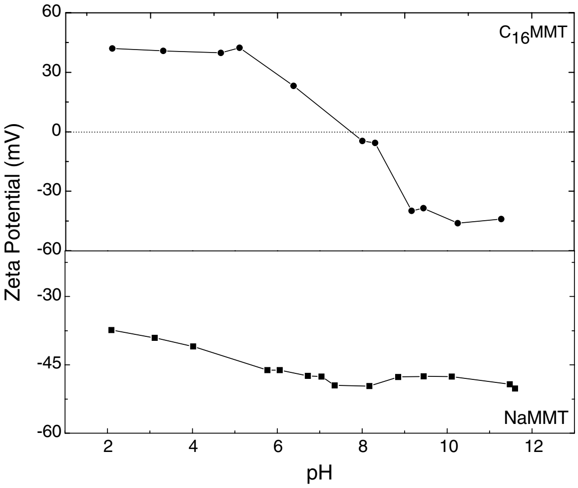

Fig. 3. Zeta potential of natural and organophilic montmorillonite as a function of pH.

3.2. Morphology of PLLA Hybrids

Fig. 4 presents XRD results for the composites formed. As mentioned earlier, the mean basal spacing of C_{16}MMT is 1.82 nm. The diffraction patterns of the composites reveal that the characteristic peak, referred to the $d_{(001)}$ of C_{16}MMT, is shifted towards lower 2θ values and is broadened indicating that polymer chains have diffused into the silicate galleries expanding the clay structure ('intercalation'). The corresponding calculated $d_{(001)}$ values change in a consistent way with the clay content of the hybrids produced; that is, decrease of the clay

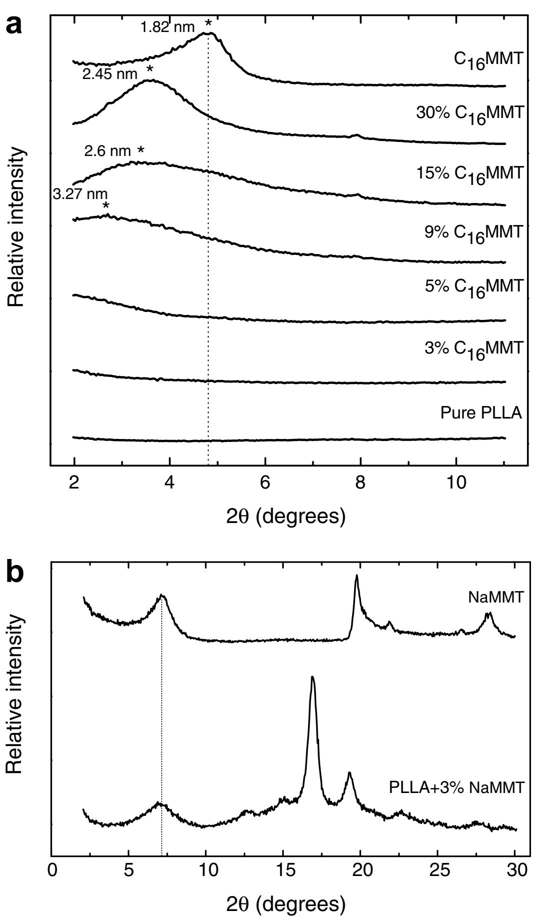

Fig. 4. X-ray diffraction patterns of (a) PLLA nanocomposites with various loadings of C_{16}MMT and (b) PLLA microcomposite with 3 wt% of NaMMT.

content increases the $d_{(001)}$ value. This means that decrease of the clay loading facilitates polymer insertion, which in turn increases the interlayer spacing. However, as more polymer enters the silicate galleries, the clay layers lose their parallel stacking and become partially disordered. The broadening of the peaks may be the result of superposition of reflections corresponding to various interlayer distances. At low clay contents, larger amounts of polymer that enter the galleries may push the platelets so far apart that the platelet separation exceeds the XRD sensitivity. The lack of peak detection for clay loadings less than 5 wt% was probably due to this high separation ('exfoliation') of the clay platelets. At low filler loading, exfoliation is the predominant mechanism of clay dispersion. Increase of the clay loading impedes complete exfoliation of such a high aspect ratio silicate sheets due to the restricted area remaining available in the polymer matrix and hence, the degree of intercalation enhances [26].

The intensity of the characteristic peak of the clay ($Id_{(001)}$) increases as the percentage of the C_{16}A-modified clay in the hybrid material becomes higher. This is because the number density of the intercalated clay particles in the polymer matrix increases, as the clay content arises, and many more X-rays are diffracted.

Mixing of the polymer with the natural, unmodified clay did not result in the formation of a nanocomposite material, as no shift of the clay's characteristic peak was observed (Fig. 4b). Usually, blending polymer matrices with NaMMT leads to the synthesis of conventional composites, since most of the polymers do not migrate into the hydrated Na^+ interlayer space due to its hydrophobicity [12].

Information arising from the XRD analysis is in good agreement with TEM observations. Fig. 5a illustrates the structure of nanocomposites with 15 wt% organophilic clay. Dark lines represent the cross sections of the clay layers and the gray area corresponds to the polymer matrix. Inspection of this picture reveals a homogeneous dispersion of the clay platelets throughout the matrix and in the nanometer-scale level. Extensive TEM observations revealed a coexistence of silicate particles in the intercalated (Fig. 5c) and the exfoliated (Fig. 5d) state for the full range of clay loadings examined.

As it is shown in Fig. 5b, TEM investigations of the composite prepared by the addition of NaMMT evidenced the existence of immiscible clay tactoids with sizes in the micrometer range. The lack of affinity between the hydrophilic silicate and the hydrophobic polymer causes agglomeration of the mineral in the polymer matrix.

The high dispersion of the organoclay in PLLA was also verified by AFM observations. The topography and phase images presented in Fig. 6a and b, respectively describe the morphology of a hybrid prepared by the addition of 9 wt% of organoclay. The height differences in the topography image and the light phase variations in the phase image indicate the presence of small and large intercalated clay tactoids dispersed into the matrix.

3.3. Thermal properties of PLLA hybrids

Fig. 7a shows TGA data for pure PLLA and its hybrids, which were taken in a N_2 atmosphere and in the temperature range of 165 °C, (where the sam-

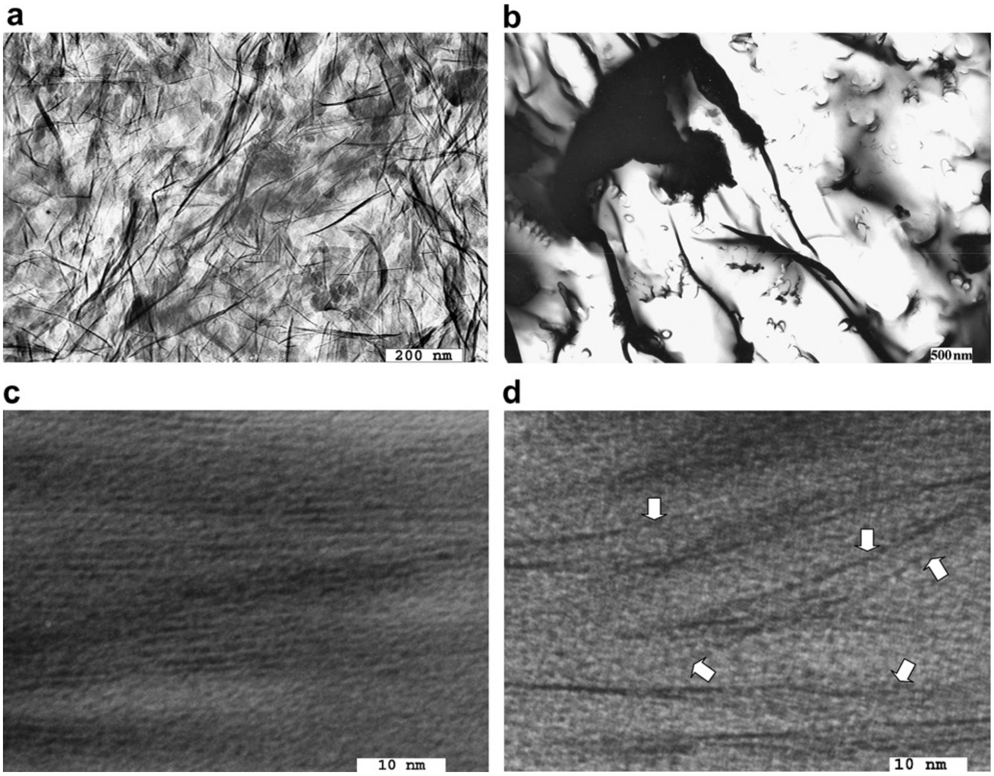

Fig. 5. TEM micrographs of PLLA with (a) 15 wt% C_{16}MMT and (b) 3 wt% NaMMT. High resolution TEM micrographs of PLLA with 15 wt% C_{16}MMT showing areas with intercalated (c) and exfoliated (d) clay platelets.

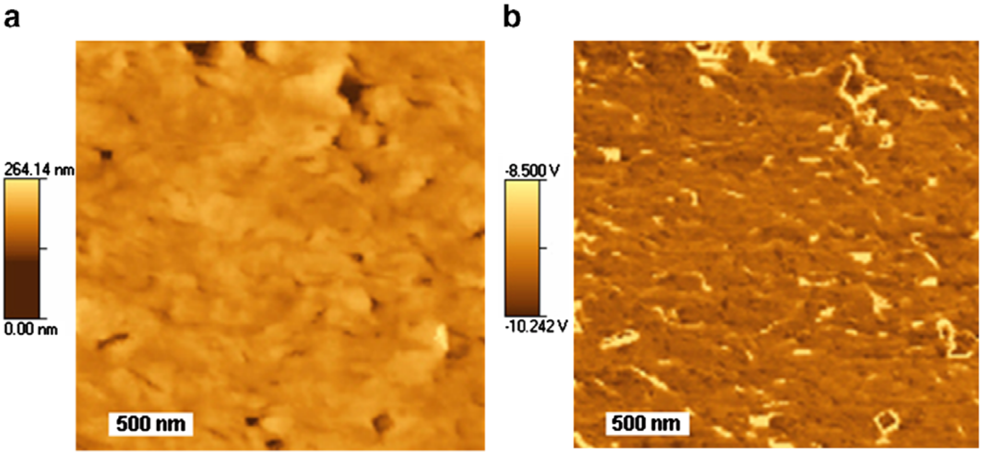

Fig. 6. AFM (a) topography and (b) phase images of PLLA nanocomposite containing 9 wt% C_{16}MMT.

ples are considered to be free of humidity), up to 750 °C. With a heating rate of 10 °C/min, PLLA volatilizes completely in a single step beginning at about 270 °C. The introduction of organophilic inorganic material improves the thermal stability of the polymer increasing the temperature of decomposition initiation, especially when the inorganic content is small. This may be attributed to the labyrinth (‘barrier’) effect originated by the high aspect ratio clay platelets, which are dispersed in the polymer matrix delaying the escape of volatile degradation products within the nanocomposite [27]. Increase of the clay loading destabilizes the polymer matrix. This can be mainly assigned to the increased

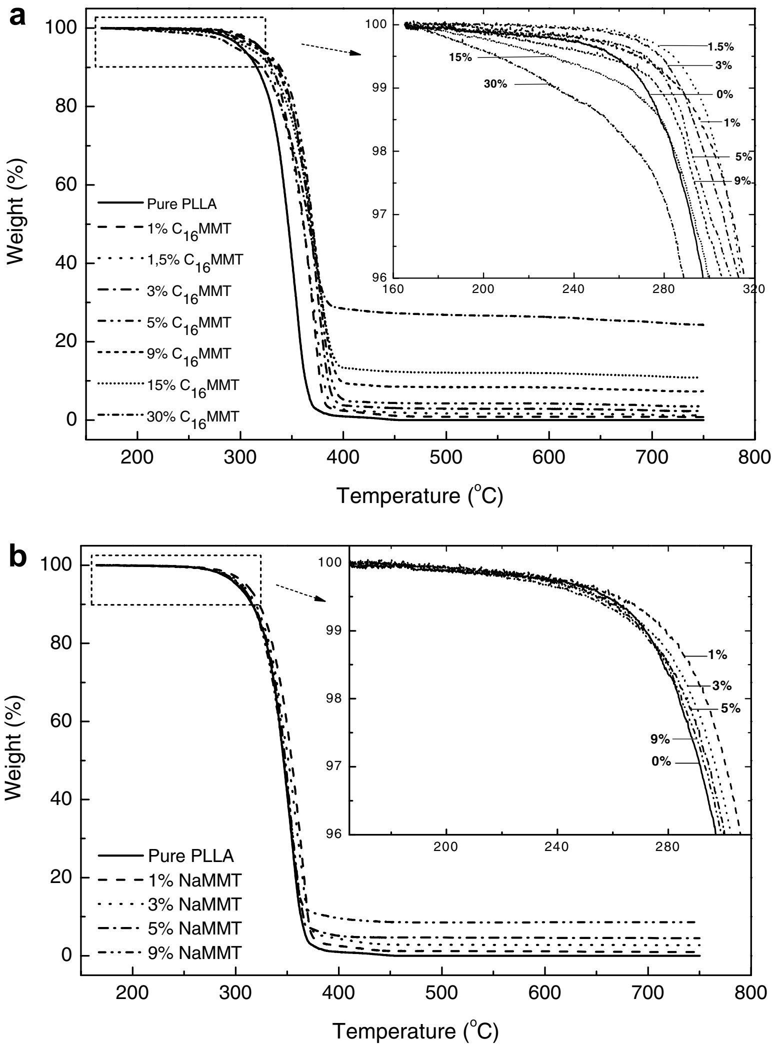

Fig. 7. TGA data for PLLA hybrids prepared with various loadings of (a) C_{16}MMT and (b) NaMMT, in inert (N_2) atmosphere.

presence of the ammonium cation, which thermally decomposes to produce ammonia and the corresponding olefin following the Hofmann mechanism [27]. As it is revealed in Fig. 8, C_{16}MMT displays a lower decomposition initiation temperature from both the natural MMT and the pristine polymer due to the ammonium cation incorporation. Therefore, when the organophilic clay is present in higher than about 9 wt% in the polymer matrix, the corresponding hybrid materials exhibit a decreased onset decomposition temperature compared to the pristine polymer due to the degradation of the organic modifier.

To support this conclusion in a more sound way and to have a concrete view about the influence of nanostructure on the polymer thermal stability, microcomposites were tested in the same TGA equipment and at the same conditions, as the ones used for the hybrid nanocomposite materials. As illustrated in Fig. 7b, the incorporation of NaMMT into the matrix does not affect the thermal degradation of the polymer significantly.

The degradation properties of the polymer/clay nanocomposites were also investigated under oxidative conditions, as shown in Fig. 9a. Oxygen induces thermal volatilization of PLLA at a lower temperature than nitrogen does. However, the organoclay addition delays the polymer mass loss significantly and, thus, increases the decomposition temperature of the hybrid material. In fact, the presence of the organophilic inorganic material enhances char formation and hinders diffusion of the volatile decom-

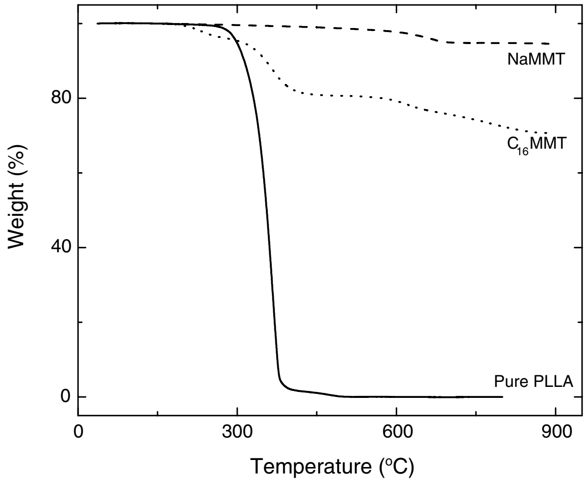

Fig. 8. TGA data for natural (NaMMT) and organophilic (C_{16}MMT) montmorillonite and pristine PLLA.

position products within the nanocomposite [4]. Moreover, the silicate platelets act as an additional barrier, which most likely works against oxygen diffusion towards the bulk of the polymer [27].

TGA data taken in oxidant atmosphere for PLLA microcomposites prepared with various loadings of NaMMT (Fig. 9b) reveal that the introduction of NaMMT to the polymer matrix resulted in a smaller enhancement of the thermal stability of the microcomposite due to the poorer dispersion of the unmodified inorganic material into the polymer matrix. The effect of the clay type and clay content on the onset decomposition temperature (that is, the temperature required for 1 wt% material mass loss) are described in Fig. 10a and b. Fig. 10a shows data taken in the presence of nitrogen (inert atmosphere), while Fig. 10b presents data taken in air (oxidant atmosphere). It appears that increased thermal stability in comparison with that of the pure polymer is observed only in the case of nanocomposites. Enhanced thermal stability in air of PLLA/MMT nanocomposites was also reported in [10].

In isothermal conditions (280 °C) under air, the polymer/clay nanocomposites lost weight with a reduced rate compared to the pure polymer, (Fig. 11a). As illustrated in Fig. 11b, the nanohybrids, prepared by the incorporation of 3–5 wt% of organically modified clay, require almost three times the time that the pure polymer needs for a 50% mass loss. This greatly retarded material volatilization may be attributed to the formation of a carbonaceous-silicate char structure, which is produced on the surface of the nanocomposite during burning [4]. In the presence of oxygen, the intimate contact between the clay platelets and the polymer favors this char formation [28], which acts as an excellent insulator and mass transport barrier that delays the diffusion of oxygen from the air to the polymer mass and slows down the escape of the volatile products generated during decomposition. Reduction in composite volume during volatilization improves this barrier property due to reassembly of the dispersed silicate layers [27].

The synergy between the polymer and the well-dispersed organo-modified silicate layers on the thermal stability of the composites can be confirmed by investigating the thermal behavior of the corresponding microcomposites at the same conditions as before (oxidant atmosphere, 280 °C). Here, volatilization was not delayed by the introduction of the NaMMT powder in the polymer matrix. This has to do with the very low clay dispersion and indicates the weak interfacial interaction between the ultrafine inorganic NaMMT particles and the matrix. A comparison of the nanocomposite (with 3 wt% C_{16}MMT) and the microcomposite (with 3 wt% NaMMT) is presented in Fig. 12, where it is clearly shown that only the former, the nanocomposite, exhibits a retarded weight loss.

Fig. 13a presents the DSC heating curves of the quenched nanocomposites. In all samples, an exothermic peak can be observed at the temperature range from 95 to 120 °C. This peak represents the crystallization of PLLA. The pure polymer crystallizes at 107 °C. Introduction of the clay nanoparticles facilitates the PLLA crystallization process during heating, leading to a decrease of the crystallization temperature. The silicate layers provide large surface area due to their nanosize and their high aspect ratio and, hence, serve as additional nucleation sites enhancing the crystallization rate of the matrix molecules [14,16,19]. This effect becomes stronger with the increase of the organomodied clay content, because of the increased presence of nucleation sites. The hybrid with 5 wt% organoclay loading displays the lowest crystallization temperature (T_c). Further increase of this content retards the crystal growth process increasing the crystallization temperature [29].

At low clay contents, the distance between the dispersed platelets is long enough, so that the additional nucleation sites that are created with the increase of the loading can easily incorporate surrounding polymer. However, when the clay loading

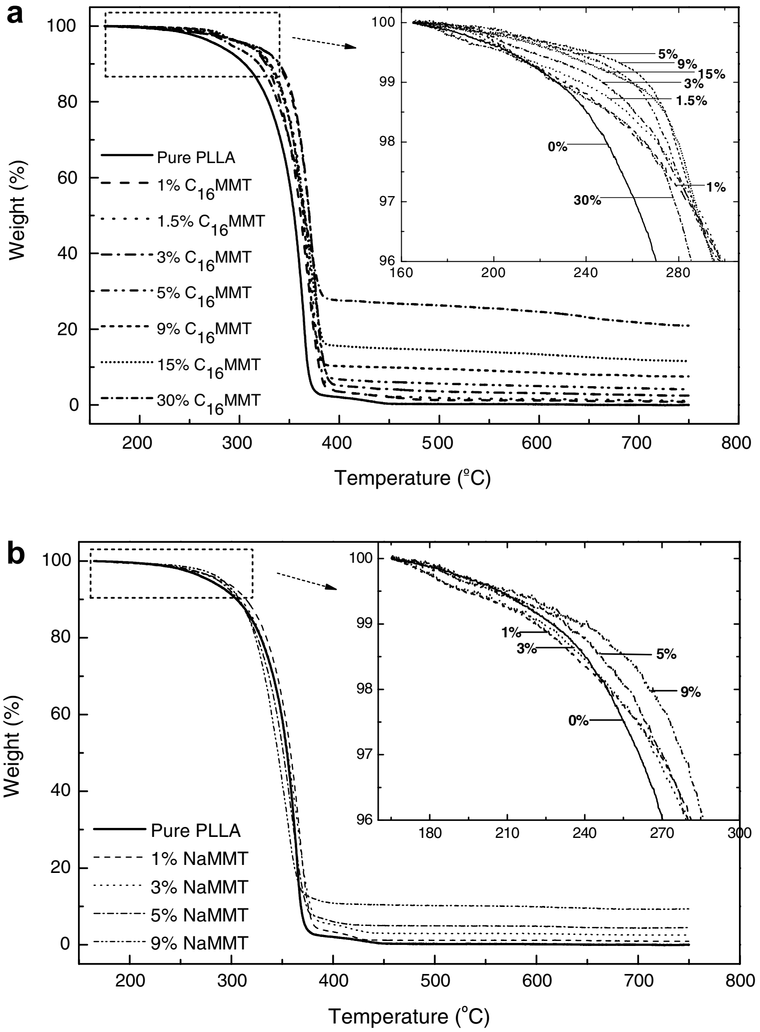

Fig. 9. TGA data for PLLA hybrids prepared with various loadings of (a) C_{16}MMT and (b) NaMMT, in oxidant (air) atmosphere.

becomes high enough, the platelets can retard crystallization acting as a physical hindrance to the diffusing polymer molecules that travel to the growing crystallite. Moreover, the high miscibility between the polymer matrix and the organic modifier and, hence, the interaction between them, partially immobilizes polymer chains attached to the clay layers and obstructs them from taking part in the flow process and, thus, the crystallization process. Therefore, the higher the concentration of the organoclay, the larger the amount of polymer which interacts with the organic modifier [14].

The incorporation of the inorganic material affects also the melting point (T_m) of the polymer. T_m is slightly decreased with increasing clay content. Besides, it is concluded that the presence of the nanoclay did not influence the glass transition temperature (T_g) of the polymer. This is in accordance with previous observations [10], where it was reported that T_g was independent of the filler concentration.

In contrast to the organophilic montmorillonite, the addition of the unmodified one to the polymer did not significantly affect the aforementioned thermal parameters, as illustrated in Fig. 13b. This result indicates the poor interaction of NaMMT with the matrix.

Fig. 14a and b present the thermal properties (T_g, T_c, T_m) of PLLA as a function of both the clay type and the clay content. It is evident that the organomodifier plays a very important role in the intimate contact between the inorganic material and the

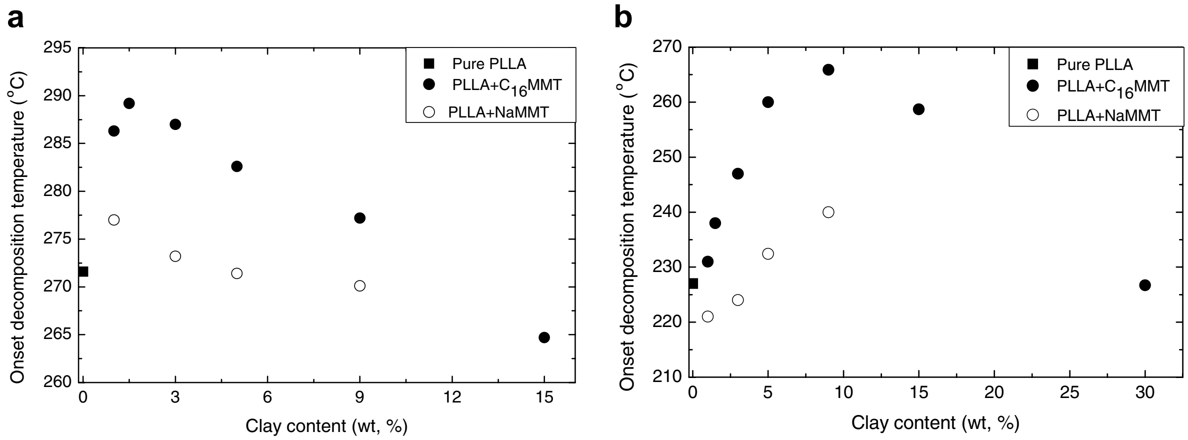

Fig. 10. Effect of clay nature and clay content on the onset decomposition temperature (1 wt% of mass loss) of the hybrid materials, in inert (a) and oxidant (b) atmosphere.

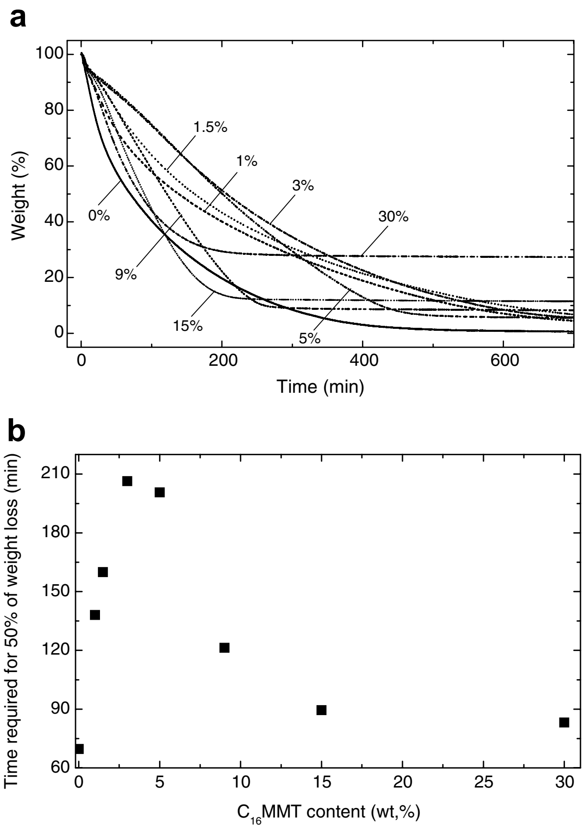

Fig. 11. (a) Effect of C$_{16}$MMT content on the weight loss of PLLA nanocomposites in oxidant atmosphere and isothermal conditions (280 °C). (b) Time required for 50% degradation of the nanocomposites.

polymer and lowers the crystallization temperature and the melting point of the polymer matrix.

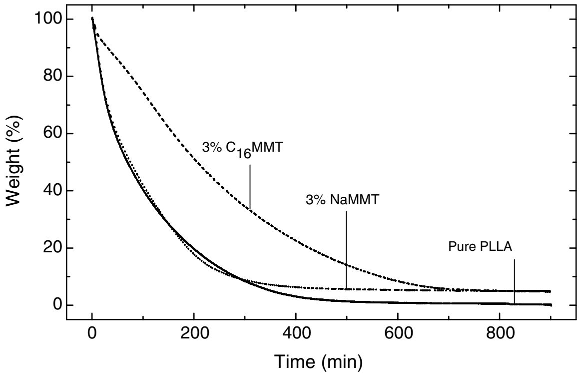

Fig. 12. TGA data in isothermal conditions (280 °C) and oxidant atmosphere for pure PLLA, nanocomposite (with 3 wt% C$_{16}$MMT) and microcomposite (with 3 wt% NaMMT) PLLA.

3.4. Mechanical behavior of PLLA hybrids

Table 1 illustrates the effect of the filler type and content on the composite's mechanical behavior. The introduction of the organoclay significantly strengthens the hybrid material. A maximum value for the strength is observed at a clay loading of 3 wt%. Further increase of the filler content hinders its dispersibility in the polymer matrix encouraging premature failure initiation. It is worth noting that the hybrid prepared by the addition of untreated montmorillonite showed higher strength compared to the pristine polymer. Similar results were also presented by Cho and Paul [2] who studied the behavior of Nylon 6 composites.

The elongation at break of the hybrids does not change significantly at very low organo-modified

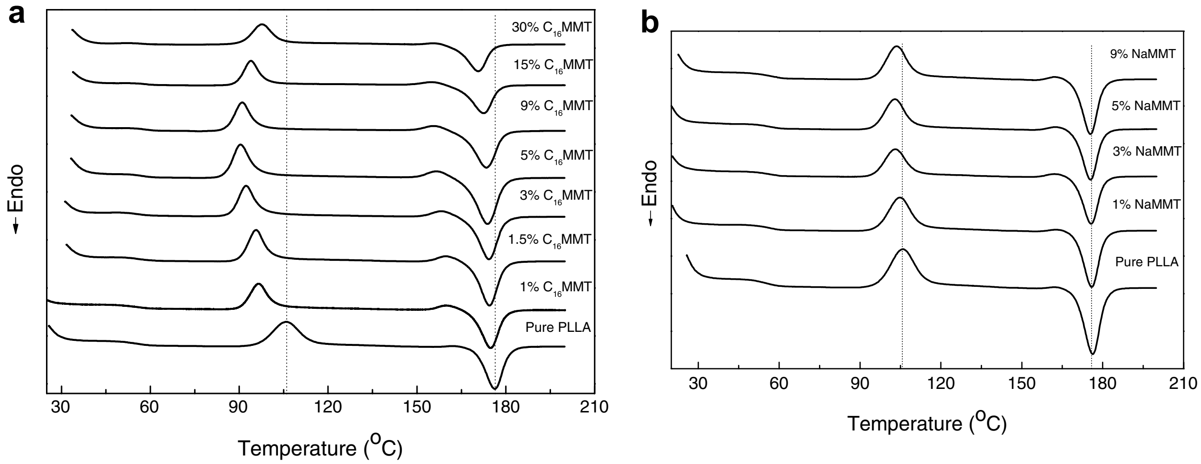

Fig. 13. DSC heating thermographs of quenched specimens of PLLA (a) nanocomposites and (b) microcomposites with various loadings of C_{16}MMT and NaMMT, respectively.

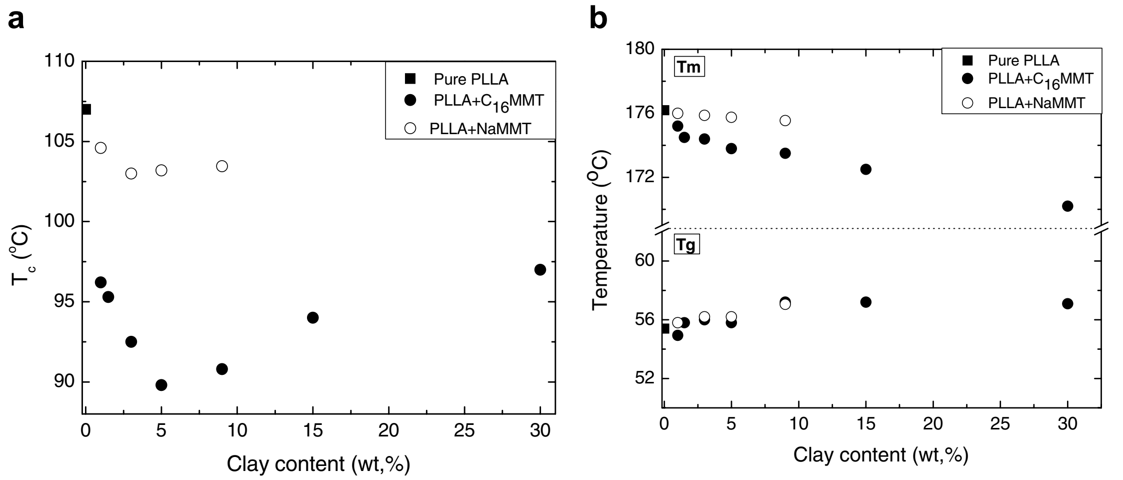

Fig. 14. Effect of clay type and clay content on (a) the crystallization temperature (T_c), (b) the glass transition temperature (T_g) and the melting point (T_m) of PLLA.

Table 1
Mechanical characteristics of the prepared hybrids

Sample	Yield strength (MPa)	Strength at break (MPa)	Elongation at break (%)	Young's modulus (GPa)
Pure PLLA	46.2 ± 0.75	35.2 ± 1.1	62 ± 4	2.05 ± 0.05
Nanocomposite PLLA				
1% C_{16}MMT	49.7 ± 0.9	41.6 ± 0.6	66 ± 9	2.29 ± 0.07
3% C_{16}MMT	52,5 ± 1	44 ± 0.53	52 ± 5	2.55 ± 0.06
5% C_{16}MMT	50 ± 0.6	43.1 ± 0.7	34 ± 2	2.81 ± 0.09
9% C_{16}MMT	48.5 ± 1.1	42.2 ± 0.8	6.5 ± 0.3	3.18 ± 0.11
Microcomposite PLLA				
1% NaMMT	48.2 ± 0.8	39 ± 0.7	50 ± 5	2.23 ± 0.1
3% NaMMT	49 ± 1.2	42 ± 0.9	30 ± 3	2.38 ± 0.1
5% NaMMT	48.4 ± 0.6	41.2 ± 0.3	10 ± 1	2.5 ± 0.06
9% NaMMT	45.4 ± 0.5	39.5 ± 0.5	4.5 ± 0.02	2.51 ± 0.08

clay content (around 1 wt%). Increase of the filler content restricts the polymer ductility leading to a rapid decrease of the elongation of the hybrid material. In fact, at low organoclay loadings (<5 wt%) exfoliation of the silicate layers prevails. The appearance of inorganic nanoparticles may restrict the molecular mobility of the surrounding matrix material leading to hybrid embrittlement [30]. Increase in clay surface area due to their nanosize and high aspect ratio can contribute to toughness enhancement provided the clay/matrix interface is sufficiently strong. Therefore, the rise in plastic deformation is expected to be larger with decreasing scale of reinforcement [31]. As the filler quantity increases, the amount of the delaminated sheets (i.e. platelets) decreases. However, the presence of non-exfoliated aggregates triggers a substantial decrease in hybrid's elongation at break. Gersappe [32] suggested that failure in polymer nanosomposites is strongly dependent on the mobility of the nanofiller particle rather than its surface area. This mobility is a complex function of the filler size, the attraction between the polymer and the filler, and the thermodynamic state of the matrix.

In the case of the conventional composites, the elongation is reduced substantially. The poor interaction between the inorganic material and the matrix leads to a low clay dispersion and inadequate polymer chain linkage to the mineral surface. Consequently, large clay aggregates formed can serve as load concentrating defects resulting in an important reduction of the material ductility. Furthermore, these agglomerates can promote the trapping of air during sample preparation leading to the formation of voids that act as damage initiation sites [33].

Even though the ASTM 1708 method is not recommended for the determination of the Young's modulus, an estimation of the composite's morphology on it can be obtained. As shown in Table 1, the presence of organoclay significantly improves the modulus of elasticity of the composite material and this modulus increases with filler content. Thus, a 50% rise of the nanocomposite's modulus can be obtained at a clay loading of 9 wt%. This may be attributed to the structure of the silicate layers, which have a high aspect ratio and a large surface area, as well as to the interaction of these ultrafine inorganic particles with the matrix. Strawhecker and Manias [34] suggested that polymer stiffens through its affinity and adhesion to the filler surfaces. Furthermore, the increase of the effective particle volume fraction caused by the increase of the interlamellar spacing within each particle may play an important role in the increase of polymer stiffness [35,36].

The introduction of the natural clay enhances the elastic modulus of the hybrid material to a lesser extent than the organoclay does. Conventional composites displayed limited modulus increment with the increase of the inorganic clay content up to 5 wt%. Beyond this loading, the additional clay particles were introduced in polymer regions that had been already affected by other montmorillonite aggregates and, thus, the Young's modulus increase was even smaller.

SEM observations of the tensile deformed composites' microstructure in the vicinity of the propagated crack affirmed a different deformation process mechanism between the two types of the composites. In the case of nanocomposites (Fig. 15a and c) 'micro' cracks were formed on the surface due to high miscibility of the organo-modified inorganic particles with the matrix and excellent adhesion with the polymer. In contrast, the conventional composites (Fig. 15b and d) displayed large cavities on the deformed surface, suggesting a deficient bonding between the non-dispersed clay particles and the polymer.

In a nanocomposite, the particle interlayer spacing is similar to or even smaller than the polymer crystalline lamellae thickness and, therefore, the polymer confined between adjacent intercalated silicate layers is usually non-crystallizable [37]. For this reason, the matrix polymer molecules inserted into the silicate galleries exhibit different properties compared to those of the bulk pristine polymer [38]. Moreover, the interaction between the silicate layers is relatively weaker than that of the PLLA/organoclay interfacial bonding strength and the cohesive strength of PLLA. Therefore, during the deformation process, microcrack initiation takes place inside the weakly bonded clay [30,37,39,40]. Accordingly, crack propagation occurs by splitting clay layers, breaking matrix ligaments and merging microcracks. This argument is also supported by the fact that micro-voids were formed between the silicate layers of some samples during the preparation for TEM observations, as shown in Fig. 16. Similar observations were also mentioned by Nair et al. [31]. Moreover, Chan et al. [41] reported that in polypropylene/$CaCO_3$ nanocomposites failure initiation occurred at the amorphous region of the polymer confined between the $CaCO_3$ particles.

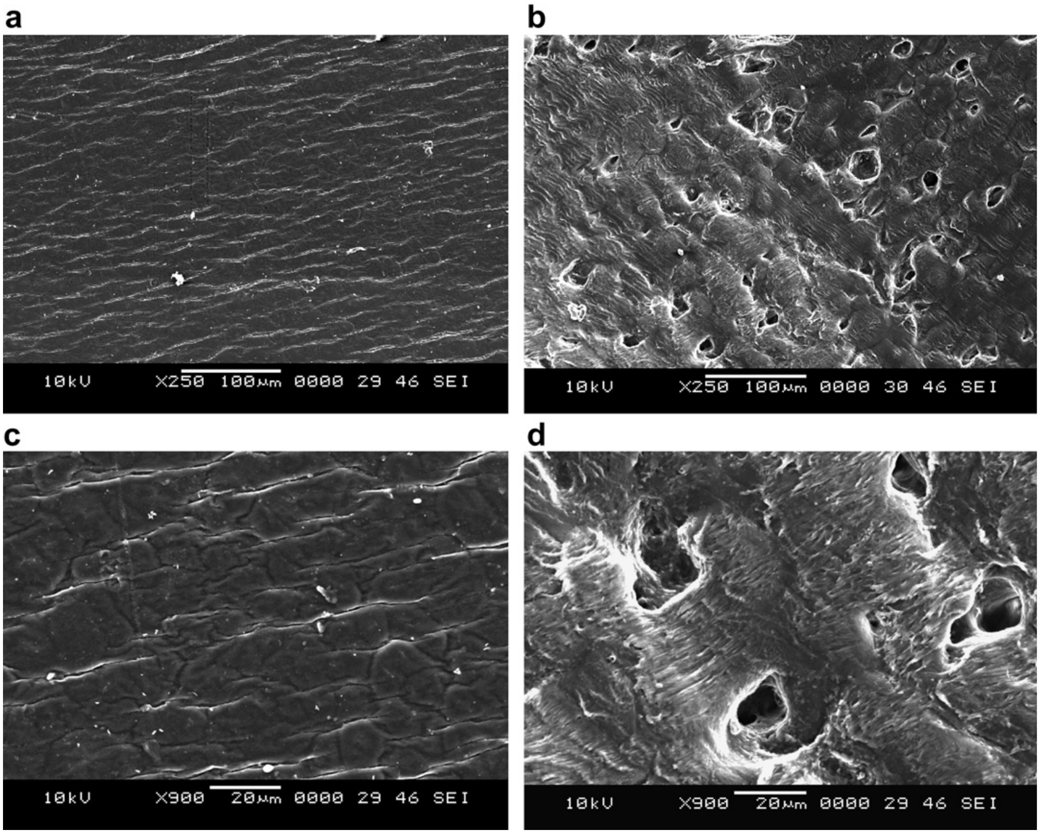

Fig. 15. SEM micrographs of the surface morphology in the vicinity of a crack of tensile deformed PLLA hybrids containing 9 wt% C_{16}MMT ((a) and (c)) and 9 wt% NaMMT ((b) and (d)).

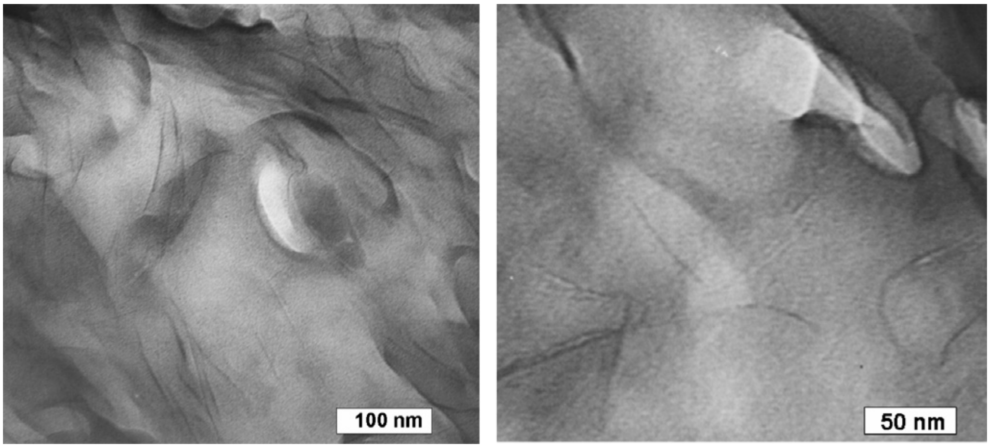

Fig. 16. TEM micrograph of the nanocomposite material containing 5 wt% C_{16}MMT. The white areas represent voids formed between silicate layers during the sample preparation process.

When a conventional composite is subject to a load, stress concentrates in the vicinity of the large non-dispersed particles due to the elastic modulus difference between the clay and the polymer. When the stress concentration reaches a critical value, void formation takes place most likely by debonding at the interface separating the unmodified clay and the matrix. This debonding is possible because the

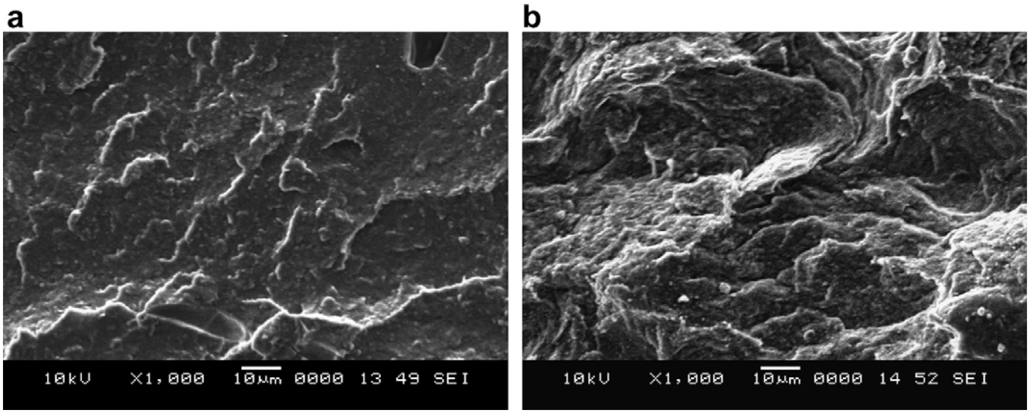

Fig. 17. SEM micrographs of the fracture surface of PLLA nanohybrids containing (a) 1 wt% and (b) 9 wt% of organo-modified MMT. The samples were broken after immersing them in liquid nitrogen.

adhesion in this interface is not due to strong interactions or chemical bonds. Larger inhomogeneities concentrate much higher stresses locally and, therefore, larger voids are formed around them. Decohesion occurring at the NaMMT/matrix interface was also reported recently [42,43] from studies of the properties of Nylon 6 nanocomposites.

The fracture surface of the nanocomposites, broken by using liquid nitrogen, has been examined by SEM. As it can be inferred from Fig. 17, increase of the organoclay content causes an increase in the fracture surface roughness of the material. When a propagating crack meets clay layers oriented perpendicular to the crack propagation direction, it may bend along the region adjoining the clay-matrix interface. As the clay concentration increases, the distance between intercalated clay particles decreases leading to a more tortuous path for the crack [40,44,45]. Consequently, the surface roughness arising from the increased path length will also increase, in accordance with the SEM observations.

4. Conclusions

The influence of the micro- and nano-structure on the thermomechanical characteristics of poly(L-lactic acid)/montmorillonite (PLLA/MMT) hybrid materials, which were prepared by the solution casting method, has been investigated. XRD, TEM and AFM studies of the nanohybrids' morphology showed that, at low clay content, exfoliation dominates. However, when the filler content exceeds 5 wt%, complete exfoliation of the high aspect ratio organo-modified MMT particles into the limited polymer mass is obstructed and a coexistence of exfoliated and intercalated clay particles is observed.

The nanocomposites display enhanced thermal stability compared to microcomposites and to pure polymer, especially in oxidant atmosphere. The dispersed inorganic platelets assist the formation of a protective layer on the surface of the polymer, which acts as an insulator and a mass transport barrier retarding the decomposition rate of the polymer matrix. Moreover, the addition of organo-modified clay leads to a decrease in the crystallization temperature (T_c) and melting point (T_m) of the matrix. The dispersed inorganic platelets serve as nucleating agents facilitating polymer crystallization. However, high clay loadings retard the overall bulk crystallization kinetics by hindering the mobility of polymer chains. The addition of the natural, unmodified clay does not have any significant effect on both thermal parameters, T_c and T_m, underlying the poor interaction between the untreated clay and the polymer matrix. In addition, there is not any consistent trend regarding the effect of the filler on the glass transition temperature (T_g) of the polymer in both the nanocomposite and the microcomposite.

The presence of organoclay results in a substantial enhancement of the nanocomposite's mechanical properties. On the contrary, the microcomposites formed by the addition of the natural clay do not show as much improvement in their mechanical properties as the nanocomposites do. The observation of the deformed surfaces in the vicinity of the crack by the use of SEM reveals a different deformation process mechanism between the nanocomposites and the microcomposites. In the first case, micro-cracks are formed possibly due to the delamination between intercalated clay layers, while the microcomposites display a big number of large cavities suggesting that a decohesion occurs at the interface between PLLA and MMT agglomerates.

Acknowledgments

The financial support of the Greek Ministry of Education and the European Union through the research grant Archimedes (MIS 86383) is gratefully acknowledged.

The help of Veeco Co. is also acknowledged and especially that of Drs. Hartmut Stadler, Natalia Erina and Rian Li, who took the AFM images.

References

[1] Ray SS, Okamoto M. Prog Polym Sci 2003;28:1539.
[2] Cho JW, Paul DR. Polymer 2001;42:1083.
[3] Lu CS, Mai YW. Phys Rev Lett 2005;95:088303.
[4] Gilman JW, Jackson CL, Morgan AB, Harris R, Manias E, Giannelis EP, et al. Chem Mater 2000;12:1866.
[5] Jang BN, Costache M, Wilkie CA. Polymer 2005;46:10678.
[6] Ray SS, Bousmina M, Okamoto K. Macromol Mater Eng 2005;290:759.
[7] Ikada Y, Tsuji H. Macromol Rapid Comm 2000;21:117.
[8] Drumright RE, Gruber PR, Henton DE. Adv Mater 2000;12:1841.
[9] Shi H, Lan T, Pinnavaia TJ. Chem Mater 1996;8:1584.
[10] Pluta M, Galeski A, Alexandre M, Paul MA, Dubois P. J Appl Polym Sci 2002;86:1497.
[11] Moraru VN. Appl Clay Sci 2001;19:11.
[12] LeBaron PC, Wang Z, Pinnavaia TJ. Appl Clay Sci 1999;15:11.
[13] Giannelis EP. Adv Mater 1996;8:29.
[14] Di YW, Iannace S, Di Maio E, Nicolais L. J Polym Sci Part B-Polym Phys 2005;43:689.
[15] Nam PH, Ninomiya N, Fujimori A, Masuko T. Polym Eng Sci 2006;46:39.
[16] Nam JY, Ray SS, Okamoto M. Macromolecules 2003;36:7126.
[17] Chang JH, An YU, Cho DH, Giannelis EP. Polymer 2003;44:3715.
[18] Krikorian V, Pochan DJ. Chem Mater 2003;15:4317.
[19] Lee JH, Park TG, Park HS, Lee DS, Lee YK, Yoon SC, Nam JD. Biomaterials 2003;24:2773.
[20] Strawhecker KE, Kumar SK, Douglas JF, Karim A. Macromolecules 2001;34:4669.
[21] Lagaly G. Solid State Ionics 1986;22:43.
[22] Hackett E, Manias E, Giannelis EP. J Chem Phys 1998;108:7410.
[23] Swartzen Sl, Matijevi E. Chem Rev 1974;74:385.
[24] Xu SH, Boyd SA. Environ Sci Technol 1995;29:312.
[25] Zhang ZZ, Sparks DL, Scrivner NC. Environ Sci Technol 1993;27:1625.
[26] Paul MA, Alexandre M, Degee P, Henrist C, Rulmont A, Dubois P. Polymer 2003;44:443.
[27] Zanetti M, Camino G, Reichert P, Mulhaupt R. Macromol Rapid Comm 2001;22:176.
[28] Berta M, Lindsay C, Pans G, Camino G. Polym Degrad Stabil 2006;91:1179.
[29] Fornes TD, Paul DR. Polymer 2003;44:3945.
[30] Gam KT, Miyamoto M, Nishimura R, Sue HJ. Polym Eng Sci 2003;43:1635.
[31] Nair SV, Goettler LA, Lysek BA. Polym Eng Sci 2002;42:1872.
[32] Gersappe D. Phys Rev Lett 2002;89:058301.
[33] Singh RP, Zhang M, Chan D. J Mater Sci 2002;37:781.
[34] Strawhecker KE, Manias E. Chem Mater 2000;12:2943.
[35] Kornmann X, Thomann R, Mulhaupt R, Finter J, Berglund L. J Appl Polym Sci 2002;86:2643.
[36] Sheng N, Boyce MC, Parks DM, Rutledge GC, Abes JI, Cohen RE. Polymer 2004;45:487.
[37] Dennis HR, Hunter DL, Chang D, Kim S, White JL, Cho JW, Paul DR. Polymer 2001;42:9513.
[38] Vaia RA, Sauer BB, Tse OK, Giannelis EP. J Polym Sci Part B-Polym Phys 1997;35:59.
[39] Dasari A, Yu ZZ, Mai YW, Hu GH, Varlet JL. Compos Sci Technol 2005;65:2314.
[40] Wang K, Chen L, Wu JS, Toh ML, He CB, Yee AF. Macromolecules 2005;38:788.
[41] Chan CM, Wu JS, Li JX, Cheung YK. Polymer 2002;43:2981.
[42] Masenelli-Varlot K, Reynaud E, Vigier G, Varlet J. J Polym Sci Part B-Polym Phys 2002;40:272.
[43] Xie SB, Zhang SM, Zhao B, Qin HL, Wang FS, Yang MS. Polym Int 2005;54:1673.
[44] Zerda AS, Lesser AJ. J Polym Sci Part B-Polym Phys 2001;39:1137.
[45] Lee J, Yee AF. Polymer 2000;41:8363.